

# Source- and Site-Specific Earthquake Ground Motions

## Application of a State-of-the-Art Evaluation Method

Takashi Nagao

Research Center for Urban Safety and Security  
Kobe University  
Kobe City, Japan  
nagao@people.kobe-u.ac.jp

Yasuhiro Fukushima

Department of Disaster Mitigation and Facility Maintenance  
Eight-Japan Engineering Consultants Inc.  
Okayama City, Japan  
fukushima-ya@ej-hds.co.jp

**Abstract**—Seismic codes stipulate earthquake ground motions by considering the seismicity and seismic amplification properties of the ground at the target site. However, the effects of source, path, and site amplification characteristics are not sufficiently anticipated in seismic codes. Regarding the source and path characteristics, earthquakes that have the strongest influence on the target site should be considered specifically, and, concerning seismic amplification, the effects of not only a shallow subsurface but also a deep subsurface should be considered. This article takes the design spectra of Japanese highway bridges as an object and compares them with the spectra produced by a ground motion prediction equation and the source- and site-specific spectra evaluated using a state-of-the-art method. The results show that the spectra differ greatly. In this way, the necessity of the application of a state-of-the-art technique in the evaluation of source, path, and site amplification characteristics is demonstrated.

**Keywords**—earthquake ground motion; site amplification factor; strong-motion simulation

### I. INTRODUCTION

Earthquake Ground Motion (EGM) is affected by source, path, and site characteristics. Codes of practice take those characteristics into account in various ways when developing principles of seismic design. Regarding the first two characteristics, AASHTO design specifications for bridges [1] and NEHRP-recommended seismic provisions for buildings [2] apply site-specific hazard analyses to reflect the effects of source and path characteristics on EGMs. Eurocode 8 [3] classifies the seismicity of the site according to the surface wave magnitude of the associated earthquake, and design coefficients for EGMs are specified according to the seismicity of the site of interest. The Japanese Specifications for Highway Bridges (JSHB) [4] classify the focal mechanisms of earthquakes into inter-plate earthquakes and shallow crustal (inner-plate) earthquakes, as well as specify the EGMs for each focal mechanism. The EGMs are then multiplied by a region coefficient according to the seismicity of the site of interest. The Japanese technical standard for buildings also specifies EGMs and region coefficients [5]. One of the problems in the application of hazard analysis when evaluating EGMs for

seismic design is that the analysis only provides a probabilistic EGM corresponding to the magnitude of reference earthquakes. Therefore, specific source characteristics such as directivity effects due to the rupture process in the fault plane [6] cannot be considered. The EGM recommendations of the JSHB are also not site-specific, because data of massive earthquakes obtained from all over the country are used. Regarding the site amplification characteristic, almost all the seismic codes and Ground Motion Prediction Equations (GMPEs) consider the amplification only in relation to a shallow subsurface. AASHTO, NEHRP, and Eurocode 8 classify site conditions according to surface soil types and  $V_s30$ , which is the average shear-wave velocity of the top 30m of the site. The JSHB and Japanese building codes classify ground conditions in accordance with the natural period of the shallow subsurface, from the ground surface down to the engineering bedrock. Here, engineering bedrock is a stiff soil whose shear-wave velocity exceeds 300m/s. It has been observed that the effect of a deep subsurface should be considered [7–10] and an evaluation of the amplification of shallow subsurfaces alone greatly underestimates the amplification values at the relevant sites [9, 10].

Recent achievements in the field of earthquake engineering have enabled the introduction of strong-motion simulation techniques such as a semi-empirical method using a characterized source model [11, 12]. When conducting a strong-motion simulation, evaluation of source, path, and site amplification characteristics by using a state-of-the-art method is very important for source- and site-specific EGMs. This study aims to address the necessity of the appropriate consideration of the said characteristics for EGMs by showing the difference in EGMs evaluated via conventional methods and those evaluated by a state-of-the-art method.

### II. CONVENTIONAL EGM

#### A. EGM in the JSHB

The JSHB stipulate six types of EGM as the maximum credible EGM at the target site, namely, the combination of two kinds of source characteristics (the inter-plate type and the inner-plate type) and three kinds of ground conditions.

Regarding earthquake type, inter-plate type EGMs were defined in relation to the 1923 Kanto Earthquake, the 2003 Tokachi-oki Earthquake, and the 2011 off the Pacific coast of Tohoku Earthquake. Inner-plate type EGMs were defined in relation to the 1995 Kobe Earthquake. The standard EGMs are multiplied by a region coefficient in the range of 0.7–1.2. Although the region coefficient is used to reflect the seismicity of the site of interest, there has been no reported evidence supporting that value. The ground condition is classified by the natural period of the shallow subsurface, as shown in Table I. Figure 1 shows the standard 5% damped EGMs.

TABLE I. GROUND TYPE CLASSIFICATION

| Ground type | Natural period $T$ (s) |
|-------------|------------------------|
| Type I      | $T < 0.2$              |
| Type II     | $0.2 \leq T < 0.6$     |
| Type III    | $0.6 \leq T$           |

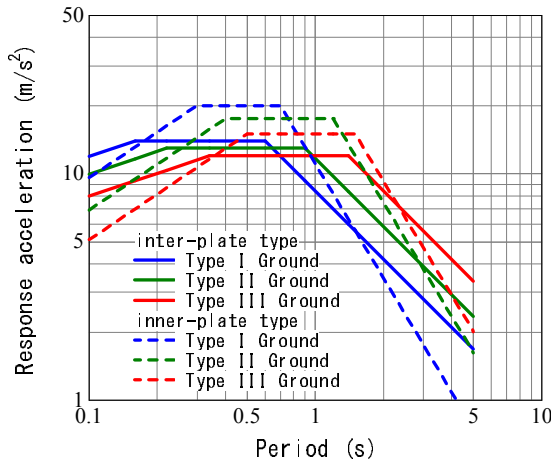


Fig. 1. Standard EGMs.

### B. GMPEs

GMPEs are widely used to evaluate EGMs in accordance with the magnitude of the reference earthquake and the surface condition of the target site. Many GMPEs have been proposed to date [13, 14]. This study employs the GMPE proposed by [13], wherein EGM is calculated by:

$$\ln(S_a(T)) = aM_W + bX - \ln(X + c \exp(dM_W)) + e(h - h_c)\delta_h + F_R + S_I + S_S + S_{SL} \ln(X) + C_k + S_{MSR} \quad (1)$$

where  $S_a(T)$  is the 5% damped response spectrum ( $\text{cm/s}^2$ ),  $M_W$  is the moment magnitude,  $X$  is the shortest fault distance (km),  $h$  is the focal depth (km), and  $\delta$  is a dummy variable equal to 0 for  $h < h_c$  and 1 for  $h \geq h_c$ , with  $h_c$  as a depth constant.  $a$ ,  $b$ ,  $c$ ,  $d$ , and  $e$  are the regression coefficients for the period  $T$ (s).  $F_R$ ,  $S_b$ , and  $S_S$  are the source type coefficients, where  $F_R$  is applied to a reverse fault-type inner-plate earthquake,  $S_I$  is applied to an inter-plate earthquake,  $S_S$  is applied to an intra-slab earthquake, and 0 is used for all other kinds.  $S_{SL}$  is the magnitude-independent path correction term for intra-slab earthquakes,  $C_k$  is the site classification coefficient, and  $S_{MSR}$  is the correction factor of the magnitude-squared term for each source type. We refer the reader to [13] for details.

### III. TARGET SITES

Four sites from the strong-motion observation network K-NET [15] were chosen as target sites in this study: GNM001 (I), YMG019 (I), FKO011 (II), and KOC014 (III). The number in the parentheses is the ground type according to the JSHB. The reference earthquakes for each site are: an inter-plate type in the form of the Nankai Trough megathrust earthquake (also known as the Nankai Trough earthquake) for YMG019 and KOC014, an inner-plate type earthquake along the fault zone of the left bank of the Katashina River (Katashina River fault earthquake) for GNM001, and an inner-plate type earthquake along the fault zone of the north edge of the Saga Plain (Saga Plain fault earthquake) for FKO011. The region coefficients provided in the JSHB for EGMs at those sites are: 1.0 for GNM001, 0.8 for YMG019, 0.7 for FKO011, and 1.2 for KOC014 [4].

### IV. SOURCE- AND SITE-SPECIFIC EGMs

#### A. Method Overview

We applied a semi-empirical method for the evaluation of source- and site-specific EGMs. The used method is also called the statistical Green's function method [11], and we referred to [16] for the specific calculation procedures. This method divides the Strong Motion Generation Area (SMGA) in a fault plane into sub-faults and evaluates the larger EGM as the summation of the small EGMs caused by the sub-faults. An SMGA is also called the asperity in the literature. A Fourier transform of the small EGM ( $u(f)$ , Green's function) is obtained with the following equation:

$$u(f) = |S(f)| \times |P(f)| \times |G(f)| \times |O(f)| / |O(f)| \quad (2)$$

where  $S(f)$  is the source spectrum,  $P(f)$  is the path spectrum,  $G(f)$  is the site amplification spectrum,  $O(f)$  is the Fourier spectrum of the small earthquake observed at the target site, and  $f$  is the frequency.

It is emphasized that source, path, and site amplification characteristics need to be source and site specifically evaluated as will be described in the following section.

#### B. Source Characteristics

The source spectrum was obtained with reference to [17] as:

$$|S(f)| = R_{\theta\phi} \cdot FS \cdot PRTITN \cdot \frac{M_{0e}}{4\pi\rho V_s^3} \cdot \frac{(2\pi f)^2}{1 + (f/f_c)} \quad (3)$$

where  $R_{\theta\phi}$  is the radiation coefficient,  $FS$  is the amplification due to the free surface ( $=2$ ),  $PRTITN$  is a reduction factor accounting for the partitioning of energy into two horizontal components ( $=0.71$  in this study),  $M_{0e}$  is the seismic moment of the small earthquake,  $\rho$  is the density,  $V_s$  is the shear-wave velocity, and  $f_c$  is the corner frequency of the small earthquake. Corner frequency  $f_c$  is calculated based on [18, 19] as:

$$f_c = 0.66V_s / \sqrt{S_e} \quad (4)$$

where  $S_e$  is the area of the sub-fault.

The summing of the waveforms of the small earthquakes, in accordance with the rupture process, yields the waveform of the large earthquake [20, 21]. This study refers to the Government of Japan's Cabinet Office [22] for the arrangement of SMGAs and source parameters setting methods for the Nankai Trough earthquake. Figure 2 illustrates the arrangements of SMGAs and rupture starting points for YMG019 and KOCH014. The SMGAs were arranged so that the EGM were largest at the target sites. The rupture starting point was set by analyzing the estimated starting point of the previous events [22]. Figures 3 and 4 exhibit the arrangements of SMGAs and the rupture starting points for the Saga Plain fault earthquake and Katashina River fault earthquake respectively. The rupture starting points were set so that the waveforms at the target sites became as large as possible due to the directivity effect. The source parameters were set by referring to [23, 24].

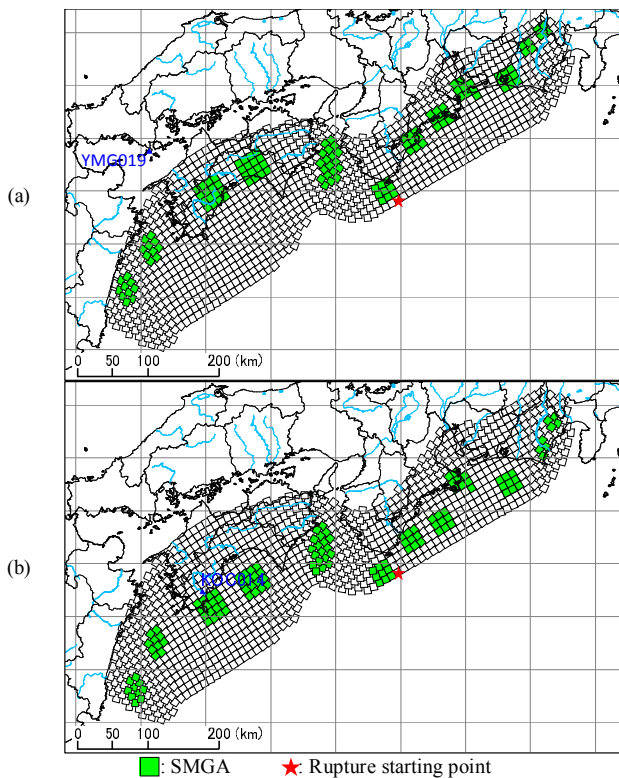


Fig. 2. Arrangements of the SMGAs and rupture starting points for the Nankai Trough earthquake: (a) for YMG019 (downdip case), (b) for KOCH014 (west case).

C. Path Characteristics

The path spectrum was obtained by [17] on the following equation:

$$|P(f)| = \frac{1}{r} \exp\left(-\frac{\pi fr}{QV_s}\right) \quad (5)$$

where  $r$  is the hypocentral distance,  $Q$  is the quality factor along the propagation path,  $V_s$  is the shear-wave velocity, and  $f$  is the frequency. The quality factor in (5), which expresses the

inelastic attenuation of seismic motion, is known to be frequency dependent and differs from area to area [25]. This study employed the quality factor proposed in previous studies by focusing on the area and earthquake types, as shown below:

- The Nankai Trough earthquake [26]:  

$$Q(f)=152f^{0.38} \quad (6)$$
- The Saga Plain fault earthquake [27]:  

$$Q(f)=104f^{0.63} \quad (7)$$
- The Katashina River fault earthquake [26]:  

$$Q(f)=166f^{0.76} \quad (8)$$

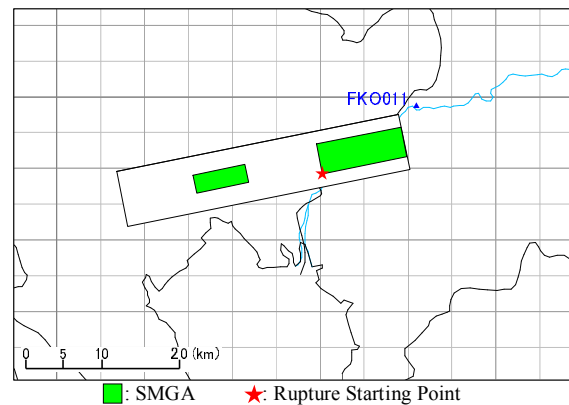


Fig. 3. Arrangements of the SMGAs and a rupture starting point for the Saga Plain fault earthquake.

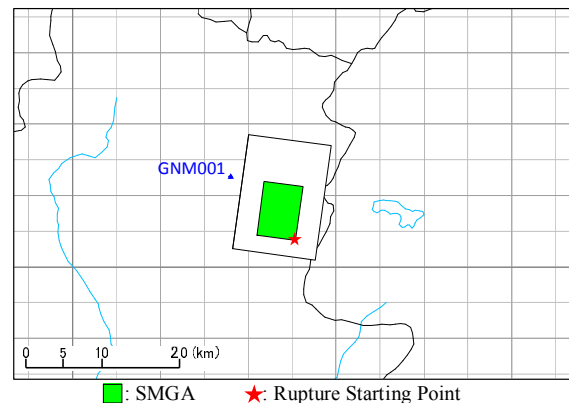


Fig. 4. Arrangement of an SMGA and a rupture starting point for the Katashina River fault earthquake.

D. Site Amplification Characteristics

Site amplification is the amplification of EGMs from the seismic bedrock to the ground surface and it is known to differ from site to site. The present study employed two kinds of site amplification factors: (i) empirically obtained site amplification factors using the spectral inversion technique [28–30] and (ii) amplification factors obtained using the multiple reflection theory and assuming a horizontally layered half-space with a vertically incident SH wave (1D amplification). Spectral inversion is a method that separates the source, path, and site amplification characteristics from the observed EGM. Site

amplification factors obtained by spectral inversion [31] are known to be larger than those obtained by 1D amplification [9], because factors affecting seismic amplification, such as 3D effects, cannot be considered in 1D amplification calculations. In addition, precise reproduction of the seismic motion by use of site amplification factors by the spectral inversion was demonstrated in [16]. In the calculation of 1D amplification, shear-wave velocity profiles from the ground surface to the seismic bedrock and quality factors were evaluated by referring to [10]. Figure 5 shows the shear-wave velocity profile at each site. Although the sediment depth at three of the sites (FKO011, GNM001, and YMG019) is almost identical (150m), the shear-wave velocity profiles above the seismic bedrock greatly differ among the sites. At KOC014, the sediment depth is 600m, which is significantly deeper than at other sites.

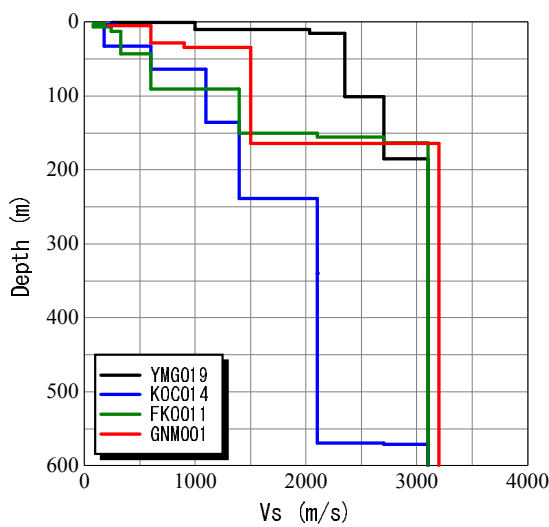


Fig. 5. Shear-wave velocity profiles.

Figure 6 compares the site amplification factors evaluated by the two methods in the range of 0.1–10Hz, as this is an important frequency range for engineering practices. For simplicity, the shallow and deep subsurface will be described as characteristics of the deep subsurface hereinafter. The black line indicates the spectral inversion, the red line denotes 1D amplification by a deep subsurface, and the green line expresses 1D amplification by a shallow subsurface. We will discuss the differences individually.

YMG019 is a hard rock site, and shear-wave velocity exceeds 2km/s at 11m depth. Thus, amplification factor observation by 1D analysis made no significant difference because the amplification factor by the shallow subsurface was unity, while the amplification factor by the deep subsurface was also unity below 1Hz and increased only a little above 1Hz. The maximum amplitude was 1.4 at 10Hz. In contrast, amplification by spectral inversion showed an amplitude of approximately 2 below 3Hz, which was larger than that demonstrated by 1D amplification. The maximum amplitude was 6.0 at 6.4Hz, which was considerably different from the results of 1D amplification.

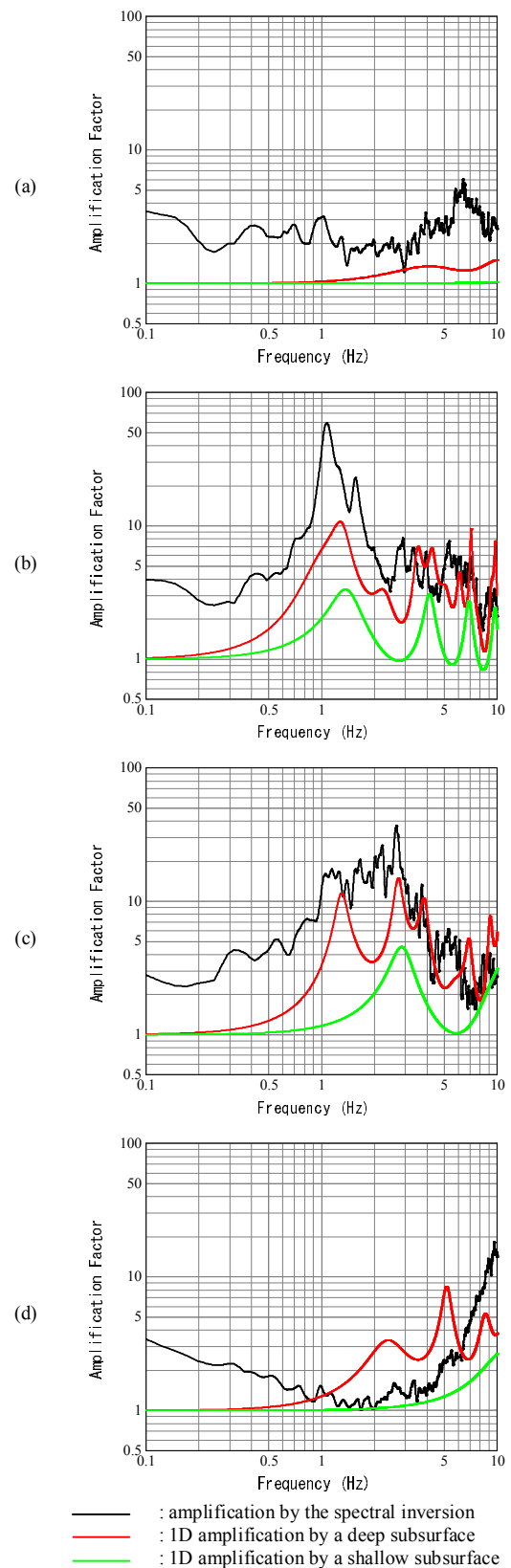


Fig. 6. Comparison of the site amplification factors: (a) YMG019, (b) KOC014, (c) FKO011, and (d) GNM001.

Concerning KOC014, the results of amplification using the three methods were similar, with a first-order peak around 1Hz, but the amplitudes were significantly different. Peak amplitudes at the first-order peak frequencies were: 60 using spectral inversion, 10 using 1D amplification with a deep subsurface, and 3.3 using 1D amplification with a shallow subsurface. The amplitude result from using spectral inversion was much larger than that obtained from using 1D analysis with a deep subsurface below 3Hz. The amplitude measurement from using 1D analysis with a shallow subsurface was much smaller than those obtained using the other two methods. Regarding FKO011, the result of the amplification factor by using spectral inversion was like that of 1D amplification with a deep subsurface, but the amplitude measurement from spectral inversion was much larger, especially below 3Hz. As with other sites, the result of 1D amplification with a shallow subsurface was much smaller than the other amplifications. GNM001 is a rock site whose shear-wave velocity is 600m/s at a depth of 10m, and it exceeds 2km/s at 130m. The 1D amplification factor by a shallow subsurface is unity below 3Hz and increased to 3 at 10Hz. 1D amplification by a deep subsurface showed peaks at 2.4, 5.1, and 8.5Hz with a maximum amplitude of 6.6 at 5.1Hz. The amplification effect above 1Hz was considerably larger when compared with that of the shallow subsurface. Amplification by spectral inversion showed a comparatively small amplitude below 4Hz and then increased to 20 at 10Hz. In summary, the site amplification factor results from using spectral inversion are larger than those from using 1D amplification with a deep subsurface. Using 1D amplification with a shallow subsurface produced the smallest results. It was inferred that the use of 1D amplification with a deep subsurface for waveform evaluation may result in an underestimation of the intensity of the EGM. It is very clear that the use of 1D amplification with a shallow subsurface alone can lead to the evaluation of EGMs on the dangerous side, thus the present study does not use the said method hereafter. Another important point to note is the difference in the amplification factors of the spectral inversion among the sites. Sediment sites (FKO011 and KOC014) show large amplitudes, whereas rock sites (YMG019 and GNM001) show small amplitudes. The difference in the amplitude is much larger than that assumed by 1D amplification. This is attributed to the 3D amplification characteristics as mentioned above.

#### E. Nonlinear Characteristics of the Shallow Subsurface

A shallow subsurface exhibits nonlinear characteristics during a strong earthquake. Therefore, the effects of nonlinear characteristics of a shallow subsurface were evaluated using the following processes: (i) obtain the input seismic motion at the engineering bedrock level via the deconvolution process using the multiple reflection theory along with the initial shear modulus of the soil (a linear earthquake response analysis), (ii) conduct an equivalent-linear earthquake response analysis [32, 33] considering the nonlinear characteristics of the soil [34], and (iii) obtain the waveform at the ground surface.

### V. RESULTS AND DISCUSSION

Figure 7 compares the horizontal, two-component (NS and EW) synthetic 5% damped calculated EGMs.

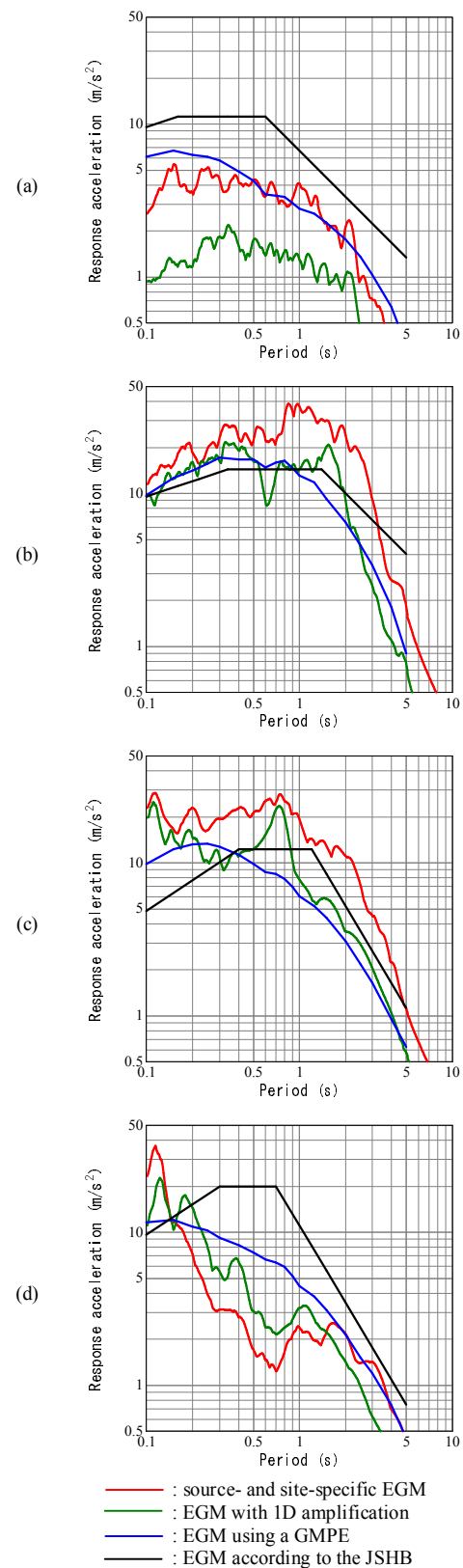


Fig. 7. Comparison of the response spectra: Nankai Trough earthquake (a) at YMG019 and (b) at KOC014, (c) Saga Plain fault earthquake at FKO011, and (d) Katashina River fault earthquake at GNM001.

Regarding EGMs for YMG019, the EGM according to the JSHB is relatively small because the region coefficient is as low as 0.8, however it still overestimates the EGM when compared with source- and site-specific EGM because the site amplification factor at YMG019 is small. IDEGM conversely underestimates EGM, and the EGM of a GMPE is generally consistent with source- and site-specific EGM. On the other hand, KOC014 is a site where the region coefficient is as large as 1.2, but because of the large site amplification factor, the JSHB underestimate the EGM when compared with source- and site-specific EGM in the period range of 3s or less. The IDEGM and GMPE results also underestimate the EGM when compared with source- and site-specific EGM. FKO011 corresponds to an area where the region coefficient is as small as 0.7. However, because the magnitude of the reference earthquake is 7.5 and the site amplification factor is large, the JSHB underestimate the EGM in the period range of 5s or less when compared with source- and site-specific EGM. The IDEGM and GMPE results also underestimate EGM. GNM001 corresponds to an area where the region coefficient is 1.0. However, the magnitude of the reference earthquake is 6.8, which is a little smaller than that of other large earthquakes, and the site amplification factor is small except in the high frequency region. Therefore, the EGM results of the JSHB overestimate the EGM when compared with source- and site-specific EGM in the period range of 0.15s or more. IDEGM also overestimates EGM in the period range of 0.15–1.5s. GMPE results also overestimate the EGM in the period range of 0.2 to 2 s.

Based on the above, it can be said that EGMs vary greatly depending on the calculation methods used. Conventional methods do not consider deep subsurface amplification and therefore often overestimate or underestimate EGM when compared with source- and site-specific EGM. For a rational EGM evaluation, it is important to evaluate the EGM source and site specifically by using the state-of-the-art method described above.

## VI. CONCLUSIONS

In this study, source- and site-specific EGM results of inter-plate and inner-plate earthquakes were estimated using a state-of-the-art method targeting various site amplification factor points and compared them with EGM results from the JSHB and GMPEs. As a result, it was made clear that although the JSHB consider the earthquake type, ground type, and region coefficients, the way it treats the source, path, and site amplification characteristics is insufficient. GMPEs are widely used to simply evaluate EGM; however, estimated EGMs may differ significantly from source- and site-specific EGM because the same three characteristics are not properly considered.

Infrastructure must be appropriately constructed and maintained, but in order to do so, the load effects on it must be appropriately evaluated, and infrastructural investments should be optimized regarding the seismic hazard at each site. Therefore, the evaluation of EGM using a state-of-the-art method is extremely important.

## ACKNOWLEDGMENT

The authors would like to thank the National Research Institute for Earth Science and Disaster Prevention, Japan for providing K-NET strong motion records and ground structure data.

## REFERENCES

- [1] *AASHTO Guide Specifications for LRFD Seismic Bridge Design (2nd Edition) with 2012, 2014 and 2015 Interim Revisions*, AASHTO, Washington, D.C., U.S.A, 2014.
- [2] *NEHRP recommended provisions for seismic regulations for new buildings and other structures*, 2000 edition, FEMA, Washington, DC, USA, 2001.
- [3] *Design of structures for earthquake resistance. Part1: general rules, seismic actions and rules for buildings*, EN-1998-1, CEN, Brussels, Belgium, 2009.
- [4] *Specifications for highway bridges, part 5, Seismic design*, ver. 2012, Japan Road Association, Tokyo, Japan: Maruzen-Yushodo Co., 2016.
- [5] T. Narafu, Y. Ishiyama, R. Ison, J. Sakuma, H. Kato, S. Kita, "Outline and features of Japanese seismic design code," presented at the *16WCEE 2017*, Santiago, Chile, Jan. 9-13, 2017.
- [6] P. G. Somerville, N. F. Smith, R. W. Graves, and N. A. Abrahamson, "Modification of empirical strong ground motion attenuation relations to include the amplitude and duration effects of rupture directivity," *Seismological Research Letters*, vol. 68, no. 1, pp. 199-222, 1997.
- [7] D. M. Boore and W. B. Joyner, "Site amplifications for generic rock sites," *Bulletin of the Seismological Society of America*, vol. 87, no. 2, pp. 327-341, 1997.
- [8] Y. Fukushima and T. Nagao, "Variation of Earthquake Ground Motions with Focus on Site Amplification Factors: A Case Study," *Engineering, Technology & Applied Science Research*, vol. 9, no. 4, pp. 4355-4360, Aug. 2019.
- [9] Y. Fukushima, T. Nagao, J. Oshige, and I. Suetomi, "Ground motion evaluation for intra-plate earthquake by different site amplification factors and source models," in *7th International Conference on Earthquake Geotechnical Engineering*, Roma, Italy, Jun. 17-20, 2019, pp. 2484-2492.
- [10] T. Nagao, "Seismic amplification by deep subsurface and proposal of a new proxy," *Engineering, Technology & Applied Science Research*, vol. 10, no. 1, pp. 5157-5163, Feb. 2020.
- [11] *Bases for design of structures—Seismic actions for designing geotechnical works*, ISO 23469:2005, 2005.
- [12] Y. Hisada, "Broadband strong motion simulation in layered half-space using stochastic Green's function technique," *Journal of Seismology*, vol. 12, no. 2, pp. 265-279, Apr. 2008, doi: 10.1007/s10950-008-9090-6.
- [13] J. X. Zhao *et al.*, "Attenuation Relations of Strong Ground Motion in Japan Using Site Classification Based on Predominant Period," *Bulletin of the Seismological Society of America*, vol. 96, no. 3, pp. 898-913, Jun. 2006, doi: 10.1785/0120050122.
- [14] T. Kanno, A. Narita, N. Morikawa, H. Fujiwara, and Y. Fukushima, "A New Attenuation Relation for Strong Ground Motion in Japan Based on Recorded Data," *Bulletin of the Seismological Society of America*, vol. 96, no. 3, pp. 879-897, Jun. 2006, doi: 10.1785/0120050138.
- [15] S. Kinoshita, "Kyoshin net (K-NET)," *Seismological Research Letters*, vol. 69, no.4, pp. 309-332, Jul./Aug. 1998, doi: 10.1785/gssrl.69.4.309.
- [16] A. Nozu, T. Nagao, and M. Yamada, "A strong motion simulation method suitable for areas with less information on subsurface structure," presented at *14WCEE*, Beijing, China, Oct. 12-17, 2008.
- [17] D. M. Boore, "Stochastic simulation of high-frequency ground motions based on seismological models of the radiated spectra," *Bulletin of the Seismological Society of America*, vol. 73, no. 6A, pp. 1865-1894, Dec. 1983.
- [18] J. N. Brune, "Tectonic stress and the spectra of seismic shear waves from earthquakes," *Journal of Geophysical Research*, vol. 75, pp. 4997-5009, Sep. 1970, doi: 10.1029/JB075i026p04997.

- [19] J. N. Brune, "Correction to tectonic stress and the spectra of seismic shear waves from earthquakes," *Journal of Geophysical Research*, vol. 76, p. 5002, 1971, doi: 10.1029/JB076i020p05002.
- [20] K. Irikura, "Prediction of strong acceleration motions using empirical Green's function," in *Proceedings of the 7th Japan Earthquake Engineering Symposium*, Tokyo, Japan, Dec. 1986, pp. 151–156.
- [21] K. Irikura, T. Kagawa, and H. Sekiguchi, "Revision of the empirical Green's function method by Irikura (1986)," (in Japanese), *Programme and abstracts, Seismological Society of Japan*, vol. 2, no. B25, Sep. 1997.
- [22] Cabinet Office, "Nankai Trough Giant Earthquake Model Study Group", (in Japanese), [Online], <http://www.bousai.go.jp/jishin/nankai/model/index.html> (accessed Apr. 18, 2020).
- [23] K. Irikura and H. Miyake, "Recipe for Predicting Strong Ground Motion from Crustal Earthquake Scenarios," *Pure and Applied Geophysics*, vol. 168, no. 1, pp. 85–104, Jan. 2011, doi: 10.1007/s00024-010-0150-9.
- [24] Ports and Harbours Bureau, Ministry of Land, Infrastructure, Transport and Tourism (MLIT), National Institute for Land and Infrastructure Management, MLIT, Port and Airport Research Institute, *Technical standards and commentaries for port and harbour facilities in Japan*, Tokyo, Japan: The Overseas Coastal Area Development Institute of Japan, 2009.
- [25] T. Satoh, H. Kawase, and T. Sato, "Statistical spectral model of earthquakes in the eastern Tohoku district, Japan, based on the surface and borehole records observed in Sendai," *Bulletin of the Seismological Society of America*, vol. 87, no. 2, pp. 446–462, Apr. 1997.
- [26] T. Satoh and Y. Tatsumi, "Source, Path, and Site Effects for Crustal and Subduction Earthquakes Inferred from Strong Motion Records in Japan," *Journal of Structural and Construction Engineering (Transactions of AIJ)*, vol. 67, no. 556, pp. 15–24, 2002, doi: 10.3130/aajs.67.15\_2.
- [27] K. Kato, "Evaluation of source, path, and site amplification factors from the K-NET strong motion records of the 1997 Kagoshima-ken-hokuseibu earthquake," *Journal of Structural and Construction Engineering (Transactions of AIJ)*, vol. 66, no. 543, pp. 61–68, 2001, doi: 10.3130/aajs.66.61\_2.
- [28] D. J. Andrews, "Objective determination of source parameters and similarity of earthquakes of different size," in *Earthquake Source Mechanics Volume 37*, S. Das, J. Boatwright, and C. H. Scholz, Eds, Washington, DC, USA: American Geophysical Union, 1986, pp. 259–268.
- [29] T. Iwata and K. Irikura, "Source parameters of the 1983 Japan Sea earthquake sequence," *Journal of Physics of the Earth*, vol. 36, pp. 155–184, Jan. 1988, doi: 10.4294/jpe1952.36.155.
- [30] J. Boatwright, J. B. Fletcher and T. E. Fumal, "A general inversion scheme for source, site and propagation characteristics using multiply recorded sets of moderate-sized earthquakes," *Bulletin of the Seismological Society of America*, vol. 81, no. 5, pp. 1754–1782, 1991.
- [31] A. Nozu, and T. Nagao, "Site amplification factors for strong-motion sites in Japan based on spectral inversion technique," (in Japanese), *Technical Note of the Port and Airport Research Institute*, no. 1102, 2005.
- [32] M. Sugito, "Frequency-dependent equivalent strain for earthquake response analysis of soft ground," *Proceedings of the IS-Tokyo, '95, The First International Conference on Earthquake Geotechnical Engineering*, Tokyo, 1995.
- [33] I. Suetomi and N. Yoshida, "Damping characteristics of soil deposits during strong ground motions," in *Proc. Second Int. Symposium on the Effect of Surface Geology on Seismic Motion*, Yokohama, Japan, Dec. 1–3, 1998, pp. 765–772.
- [34] S. Yasuda and I. Yamaguchi, "Dynamic soil properties of undisturbed samples," (in Japanese), *Proc. of 20th Annual Conference of JSSMFE*, Nagoya, Japan, Jun. 10–12, 1985, pp. 539–542.